Materials and Design xxx (2010) xxx–xxx

Contents lists available at ScienceDirect

Materials and Design

journal homepage: www.elsevier.com/locate/matdes

Hardening of an Al–Cu–Mg alloy containing Types I and II S phase precipitates

T.S. Parel *, S.C. Wang, M.J. Starink

Materials Research Group, School of Engineering Sciences, University of Southampton, Southampton SO17 1BJ, United Kingdom

ARTICLE INFO

Article history:
Received 3 August 2009
Accepted 23 December 2009
Available online xxxx

Keywords:
Strength
2024 alloy
Al–Cu–Mg
Precipitate
Dislocation

ABSTRACT

The effect of different thermo-mechanical treatments, including up to 10% cold work, on the hardness of the 2024 (Al–Cu–Mg) alloy was studied. Artificial ageing was conducted through heating at a constant rate to specific temperatures followed by rapid cooling. It was found that quenched only alloy 2024, which is found to form Type II S precipitates, possesses lower hardness compared to cold worked alloy 2024, on ageing to temperatures below 300 °C. Cold working lowers the temperature required for S phase precipitation to start while decreasing the quenching rate is seen to give higher hardness on ageing to temperatures below 200 °C. Type II S precipitate is found to result in lower hardening as compared to that due to Type I S precipitate. The reason for this is suggested to be due to the larger size of Type II S precipitate. The hardness of solution treated and subsequently cold worked and artificially aged 2024 is increased if the quenching is conducted in water at 80 °C. This effect is notable if the ageing temperature is below about 200 °C.

1. Introduction

The mechanical response of alloys is determined by the basic mechanisms for resistance to dislocation movement: precipitate strengthening, solute strengthening, grain boundary strengthening, dislocation strengthening, and in addition texture will play a role. Physically-based models of strength development in alloys have been constructed using a range of approaches. The main elements in such models are the description of the thermodynamics (equilibrium and metastable equilibrium), the kinetics of transformations and the relation between strength and micro-structure, which is determined by the interaction between dislocations and elements in the micro-structure. A basic requisite for predicting mechanical properties is a full understanding of the phases formed and the mechanisms by which they strengthen the alloy.

In heat treatable aluminium alloys such as the Al–Cu–Mg based 2024 alloy a super saturated solid solution is formed on quench cooling the sample from a high enough temperature. In these alloys, high strength is achieved by the precipitation strengthening mechanism [1–5]. A range of heating, quenching, cold working, stretching and ageing treatments are employed to create tempers which provide different levels of hardness. These alloys are used in commercial aircraft structures such as fuselage and lower wing surface due to their good damage tolerance, resistance to fatigue crack propagation and fracture toughness [6,7].

For Al–Cu–Mg alloys in the $\alpha + S$ (Al_2CuMg) phase field, strengthening is achieved in two stages. The first stage is considered to be due to Cu–Mg co-clusters [8–10] which form minutes after the high temperature solid solution is quenched (rapid hardening). Co-clusters are responsible for rapid hardening at low temperature (up to 160–200 °C). This stage accounts for around 60% of the final hardness increase due to ageing treatments. The second stage of hardening has been attributed to S precipitate formation [8,11,12]. A hardness plateau is normally found in between these two phases.

The S and S′ phases have been reported to precipitate in the form of laths with the $\{1\,2\,0\}_{Al}$ habit planes elongated along $\langle 1\,0\,0\rangle_{Al}$ direction [13]. Both phases have been suggested to possess the same orientation relationship (OR) with aluminium matrix as follows [8]:

$$[1\,0\,0]_{S(S')} \| [1\,0\,0]_{Al}, [0\,1\,0]_{S(S')} \| [0\,2\,\bar{1}]_{Al}, [0\,0\,1]_{S(S')} \| [0\,1\,2]_{Al} \quad \text{(OR1)}$$

The OR between the distorted S″ phase and the matrix was proposed as follows [14]:

$$[1\,0\,0]_{S''} \| [1\,0\,0]_{Al}, [0\,\bar{1}\,1]_{S''} \| [0\,\bar{5}\,3]_{Al}, [0\,1\,3]_{S''} \| [0\,1\,1]_{Al} \quad \text{(OR2)}$$

Based on the matrix transformation by Li and Yan [15], the OR2 is equivalent to:

$$[1\,0\,0]_{S''} \| [1\,0\,0]_{Al}, [0\,1\,0]_{S''} \| [0\,5\,\bar{2}]_{Al}, [0\,0\,1]_{S''} \| [0\,2\,5]_{Al} \quad \text{(OR2a)}$$

Since the mid 1990s, atom probe field ion microscopy (APFIM) and three-dimensional atom-probe (3DAP) have evidenced that the first stage of age hardening is due to the formation of co-clusters [9, 16–18]. Ringer et al. [16] proposed the following 3-stage precipitation sequences for the ageing of Al–Cu–Mg alloys:

SSS → Cu—Mg co-clusters → GPB zone → S

* Corresponding author.
E-mail address: m.j.starink@soton.ac.uk (T.S. Parel).

0261-3069/$ - see front matter © 2010 Elsevier Ltd. All rights reserved.
doi:10.1016/j.matdes.2009.12.048

where GPB zone stands for Guinier–Preston-Bagaryatski zone (see e.g. [8] and references therein). Where the Cu–Mg co-clusters are responsible for the initial hardening, GPB zone is the dominant precipitate at peak strengthening and the S phase appears in the softening stage.

Recent work has shown that a semicoherent phase with orthogonal structure occurs well before peak hardness is reached [4,8,19]. This phase has been alternatively designated S″ phase or GPB2.[1] The following 3-stage precipitation sequence is currently considered the best description of the precipitation sequence:

$$SSS \rightarrow Cu{-}Mg \text{ co-clusters} \rightarrow S''/GPB2 \rightarrow S$$

where the S phase is responsible for the peak strengthening. S″/GPB2 is considered to provide only limited contribution to strengthening for alloys with substantial Cu content [20].

S phase (Al_2CuMg) has been determined as orthorhombic Cmcm structure with lattice parameters $a_S = 0.400$ nm, $b_S = 0.923$ nm, $c_S = 0.714$ nm [21,22]. Recent work on alloy 2024 and 2324 (a purer version of alloy 2024 containing less Si and Fe) showed that S phase formed during artificial ageing in these alloys involves two variants: Types I and II S phase, where Type II differs from Type I in having a slightly different orientation and size [11]. The appearance of the two variants is particularly notable in Differential Scanning Calorimetry (DSC) curves of solution treated and quenched 2024, which reveals partially overlapping peaks of the two formation reactions [11]. The distinction between the two phases is important as different treatments will lead to different S phase type formed.

The main aim of this work is to compare the effects of Types I and II S precipitates on the hardness of 2024 alloys.

2. Experimental

Samples of alloy 2024 (Al–1.8at%Cu–1.6at%Mg–0.2at%Mn) were solution treated at 495 °C and subsequently cooled either by quenching in water at room temperature (WQ) or in water at 80 °C (SWQ). Subsequently selected samples were cold worked by 10% by compressing. Non-isothermal ageing and DSC experiments were conducted upon three types of samples: WQ, WQ-CW and SWQ-CW (see Table 1 for treatments).

WQ, WQ-CW and SWQ-CW samples were analysed using DSC. DSC runs from 50 °C to 550 °C were carried out at a constant heating rate of 10 °C/min. The DSC data obtained was processed by subtracting a 3rd order polynomial passing through points at which no reaction is expected [23]. The constants of the 3rd order polynomial are determined by the temperatures at which heat flow is expected to be zero. This procedure produces baselines with an accuracy that is expected to be about 10 mW/g.

DSC runs on selected samples were interrupted at specific temperatures in order to subject them to microhardness tests at room temperature. Hardness experiments were conducted using a load of 300 g with a dwell time of 15 s. To ascertain reproducibility and statistical validity 5–16 microhardness tests were performed at each condition. Microhardness test in which the difference in the lengths of the indentation diagonals is over 5% of the mean were discarded. The typical accuracy as calculated from the standard deviation in a set of hardness data divided by the square root of the number of indentations is about 4 HV.

TEM was conducted on a WQ sample heated to 300 °C; and WQ-CW sample also heated to 300 °C (see Table 1 for treatments). An ageing temperature of 300 °C was chosen as it is close to the temperature where Type II S precipitate is expected [11] to form.

Table 1
Thermomechanical treatments for DSC samples.

Designations	Treatment details
WQ	Solution treated at 495 °C for 15 min + room temperature water quenched + keep at room temperature for 10 min
WQ-CW	Solution treated at 495 °C for 30 min + room temperature water quenched + immediately cold worked by 10% + room temperature for 10 min from quench
SWC-CW	Solution treated at 495 °C for 30 min + 80C water quenched + immediately cold worked by 10% + room temperature for 10 min from quench

3. Results

Alloy 2024 was subjected to three different treatments. The DSC curves, presented in Fig. 1, reveal that during heating up to 520 °C five main reactions occur. The first stage consists of an exothermic reaction (i.e. a precipitation reaction) occurring in the WQ 2024 only, between about 60 °C and 110 °C (marked by A in the DSC thermograms). Recent research has shown that this reaction is due to Cu–Mg co-cluster formation [10,24]. Co-cluster formation is not observed in cold worked alloy 2024, which has been attributed to a lack of vacancies which are required to be present to enable Cu and Mg diffusion at these low temperatures. In cold worked materials, these vacancies are thought to be annihilated by dislocations. The second major reaction is the endothermic effect that takes place between about 160 and 230 °C. This is attributed [8,10,24] to the dissolution of co-clusters and possibly GPB2 zones. The third effect is an exothermic effect that peaks at around 250 °C and is believed to be due to Type I S precipitation. Precipitation is considered [8] to occur earlier in cold worked alloy 2024 due to an increase in dislocations that act as heterogeneous nucleation sites for the formation of Type I S phase. WQ 2024 also shows an exothermic peak representing precipitation, but this takes place at a higher temperature (due to fewer dislocations), this precipitation is again believed to be due to Type I S phase formation. The WQ samples show a shoulder in the exothermic effect at about 290 °C which indicates the occurrence of a small precipitation reaction. The precipitate formed is believed to be Type II S precipitate [12]. The WQ-CW and SWQ-CW samples do not show this ef-

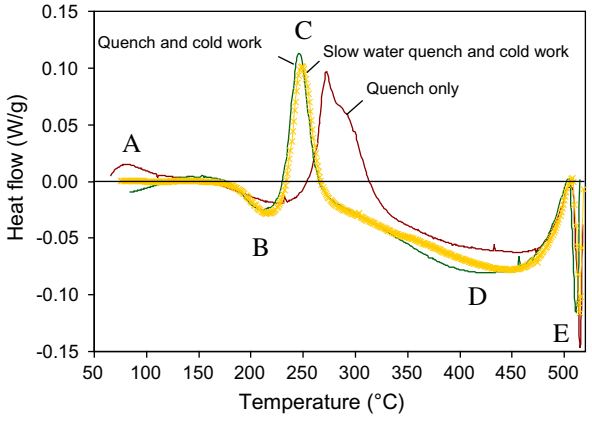

Fig. 1. DSC thermogram of quench only, room temperature water quench and cold work; and 80 °C water quench and cold work treated alloy 2024 samples.

[1] It is noted that the terms used for the various phases (identified or suggested) in Al–Cu–Mg alloys as used in the existing literature do not constitute a fully logical set of terms, see e.g. discussions in [12,18].

Please cite this article in press as: Parel TS et al. Hardening of an Al–Cu–Mg alloy containing Types I and II S phase precipitates. J Mater Design (2010), doi:10.1016/j.matdes.2009.12.048

fect. The amount of S phase formed (Types I and II) appears similar for all three treatment conditions.

The next stage, D, sees a dissolution reaction. Here, the S phase precipitates dissolve back into the aluminium matrix [25]. At temperatures in excess of about 400 °C, the DSC thermograms for all the samples studied tend to converge. This is because the rate of dissolution will be mostly determined by thermodynamic equilibrium and heating rate. The last stage, E, takes place after 505 °C and shows a sharp endothermic effect which is due to the partial melting of S + θ eutectics [23].

TEM with selected area diffraction (SAD) on WQ 2024 aged at 300 °C (Fig. 2) showed $\langle 1\,0\,0\rangle_S$, $\langle 0\,2\,1\rangle_S$ and $\langle 0\,1\,3\rangle_S$ variants of the S phase [8]. The bright field image indicates the presence of at least 2 phases in the aluminium matrix. The larger phases seen in Fig. 2a are known to be T phase ($Al_{20}Cu_2Mn_3$) dispersoids [8], which are commonly found in aluminium alloys containing Mg, Cu and Mn. The SAD patterns obtained from the smaller precipitates are consistent with S phase. However, the precipitates are too small to allow a diffraction pattern from a single precipitate that has sufficient resolution to determine whether they are Type I or Type II S precipitate.

A typical bright field TEM micrograph obtained for WQ-CW 2024 aged to 300 °C is shown in Fig. 3. Again T phase ($Al_{20}Cu_2Mn_3$) dispersoids are present, and the smaller precipitates are S phase. Comparison of Figs. 2a and 3 shows that the S precipitates in WQ-CW 2024 aged to 300 °C are smaller and more homogeneously distributed as compared to the WQ sample aged to 300 °C.

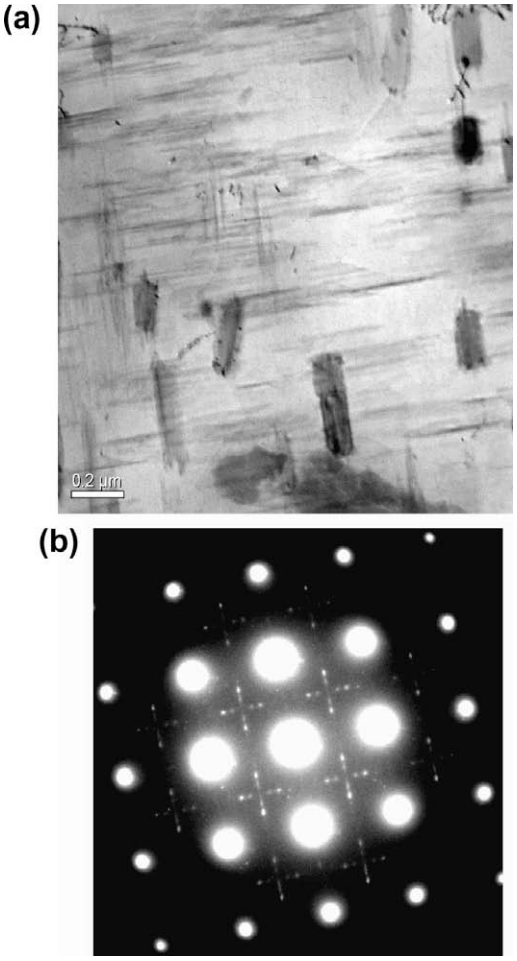

Fig. 2. TEM bright field micrograph (a) and SAD (beam direction [1 0 0]) encompassing a number of the smaller precipitates in $[0\,0\,1]_{Al}$ direction (b) of WQ 2024 aged to 300 °C. The larger particles of lengths ranging 0.2–0.8 μm are T phase dispersoids. SAD is consistent with $\langle 100\rangle_S$, $\langle 021\rangle_S$ and $\langle 013\rangle_S$ variants in the Al matrix.

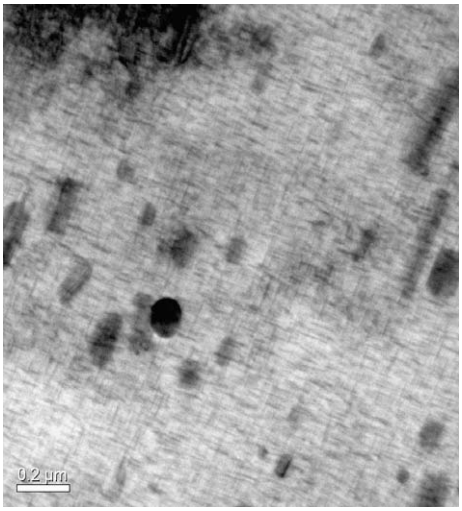

Fig. 3. TEM micrograph of quenched and cold worked alloy 2024 aged to 300 °C, showing the fine S phase precipitates and the larger rod shaped T phase dispersoids (typical diameter 0.1–0.2 μm).

Fig. 4 shows the room temperature hardness of WQ, WQ-CW and SWQ-CW 2024 after heating at 10 °C/min to the target temperature indicated. It is apparent that the hardness of the WQ sample increases on heating from 50 to 100 °C. Thereafter the strength is seen to change little up to 250 °C. The hardness after heating to 300 °C is seen to be slightly less than that after heating to 250 °C while the decrease during 50 °C intervals is higher at 350 °C and 400 °C and less so at 450 °C. WQ-CW and SWQ-CW 2024 display similar hardening with temperature. The only notable difference is that SWQ-CW 2024 shows a slightly higher hardness for treatments up to about 150 °C. The highest hardness is seen in the WQ-CW alloy after treatment at 250 °C. WQ 2024 is seen to be softer than the other treatments but the difference diminishes for treatments higher than 300 °C. After this temperature all treatments seem to show similar hardening with temperature.

4. Discussion

To appreciate the increment in critical resolved shear stress (CRSS) due to rod shaped precipitates like the present S phase precipitates we can apply strengthening theories such as in [25]. The total CRSS of the grains ($\Delta\tau_{tot}$) can be approximated well by the

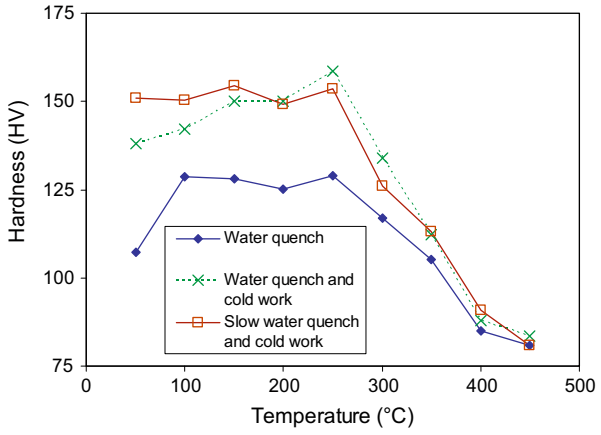

Fig. 4. Temperature hardening curve of quenched only; quenched and cold worked; and slow water quenched and cold worked alloy 2024.

Please cite this article in press as: Parel TS et al. Hardening of an Al–Cu–Mg alloy containing Types I and II S phase precipitates. J Mater Design (2010), doi:10.1016/j.matdes.2009.12.048

phenomenological Pythagorean and linear superposition approximations, which are used for summation of the obstacle strengths of similar and different magnitudes [3,25]:

$$\Delta\tau_{tot} = \Delta\tau_{ss} + \sqrt{\Delta\tau_s^2 + \Delta_{cl}^2 + \Delta_d^2} \quad (1)$$

where $\Delta\tau_{ss}$ and $\Delta\tau_d$ are the increase in CRSS of the grains due to the solute in the matrix and the dislocations, respectively. The yield strength is proportional to $\Delta\tau_{tot}$, and the hardness is approximately proportional to the yield strength. Evaluation of the different strengthening contributions has been performed [4,10,25,], which show that for heat treatments in the range of about 230–330 °C strengthening due to (variants of) the rod shaped S phase is dominant.

WQ 2024 shows an increase in hardness on increasing the temperature to 50–100 °C followed by a slight decrease at 150 °C and 200 °C. This corresponds well with DSC observations that show an apparent co-cluster precipitation peak at 100 °C. The DSC thermograms show co-cluster formation decreases after this point and dissolution is seen to occur after 150 °C. This is thought to be the main reason for the reduction in hardness at 200 °C. Co-cluster dissolution is seen to reach a maximum before 250 °C and Type I S phase precipitation is seen to start to occur at around this temperature. This explains why an increase in hardness is seen at 250 °C. Type I S precipitation is seen to peak between 250 °C and 300 °C. The slight decrease in hardness at 300 °C could be due to the conversion of Type I S precipitate into Type II S precipitate which occurs at this temperature as Type II S precipitate is found to be coarser.

WQ-CW 2024 shows an increase in hardness from 50 °C to 150 °C (Fig. 4). This increase, however, is not as large as observed in WQ 2024 (i.e. in the absence of cold work). This is though to be due to the strong reduction in co-cluster formation in the cold worked samples as indicated in the DSC thermograms (Fig. 1). At 200 °C, dissolution (possibly dissolution of a limited amount of co-clusters that may still have formed) is seen and further hardening is not observed at this temperature. Type I S phase formation rate is seen at around 250 °C which as expected coincides with the peak hardness value observed for this treatment. Here a high density of Type I S phase is believed to be present in the aluminium matrix, making dislocation motion more difficult. From 300 °C onwards a large decrease in hardness is observed due to S phase coarsening and dissolution [25].

SWQ-CW 2024 shows larger hardness when heated to between 50 °C and 150 °C than either of the other two treatments (see Fig. 4). This is thought to be due to the combination of cold work, which causes work hardening, and the prior quench to 80 °C which is expected to cause the formation of co-cluster during the later stages of the slower quench and during the brief spell at 80 °C. It is also clear from Fig. 4 that the difference in hardening decreases with temperature indicating that annealing of dislocations (i.e. recovery) and possibly even recrystallisation, combined which S phase coarsening and dissolution reduces any hardness differences.

All the temperature hardening curves show a decrease in hardness at 200 °C due to a dissolution reaction (possibly co-cluster dissolution). The DSC thermograms of cold worked samples in Fig. 1 reveal that the amount of S phase formed is less when quenching rate is decreased. This effect is seen to lower the hardening observed in SWQ 2024 after heating to 250 °C. Comparing WQ-CW 2024; and WQ-SWQ 2024 it is apparent that decreasing the quenching rate leads to a shift in the peak hardness from 250 °C to 150 °C. Lowering the quenching rate is expected to lead to less dissolved alloying elements in the aluminium matrix that are available for precipitation during subsequent (isothermal on non-isothermal) ageing and hence less solute will be available for forming hardening phases. This explains the low hardening increments in increasing the heat treatment from 100 °C to 250 °C.

A hardness peak is observed for heating to 250 °C for all treatments. This confirms that the formation of Type I S precipitate leads to an increase in the hardness of alloy 2024. The decrease in hardness at 300 °C for quenched alloy 2024 reveals that Type II S precipitate has a lower hardening effect than Type I S precipitate. Furthermore, the hardness at 300 °C due to the formation of Type II S precipitate is still slightly less than the hardness of cold worked alloy 2024 at the same temperature even though the latter starts to experience Type I S phase dissolution and possibly coarsening at this temperature. The reason for the lower strength of alloy 2024 containing Type II S precipitate is due to this precipitate being larger than Type I S precipitate. Quench only alloy 2024 shows a wider S phase precipitation reaction taking place possibly due to the formation Type II S phase.

S phase dissolution starts to take place at around 300 °C for cold worked samples and between 300 °C and 350 °C for quenched only treatment (see Fig. 1). Again this difference in temperatures is due to the larger number of dislocations present in cold worked alloy 2024 which act as nucleation sites that allow phase transformation to take place at lower temperatures. This stage of dissolution leads to softening of alloy 2024 as the number of S phase precipitates decreases. At around 450 °C the rate of softening of alloy 2024 decrease because as indicated by the DSC thermograms, S phase dissolution is nearly complete.

5. Conclusions

This study reveals the effect of Type II S precipitate on the strength of 2024 alloy as follows:

1. The strength of alloy 2024 containing Type II S precipitate, i.e. quenched only, is substantially less than that obtained through treatments involving cold work. Hence Type II S precipitate are generally not desirable for structural applications.
2. The hardness of solution treated and subsequently cold worked and artificially aged 2024 is increased if the quenching is conducted in water at 80 °C, a slower quench. This effect is notable if the ageing temperature is below about 200 °C.

References

[1] Shih HC, Ho NJ, Huang JC. Metall Mater Trans 1996;A27:2479–94.
[2] Liu G, Zhang GJ, Ding XD, Sun J, Chen KH. Mater Sci Eng A 2003;344:113–24.
[3] Khan IN, Starink MJ, Yan JL. Mater Sci Eng A 2008;472:66–74.
[4] Wang SC, Starink MJ, Gao N. Scr Mater 2006;54:287–91.
[5] Zainul Huda, Nur Iskandar Taib, Tuan Zaharinie. Mater Chem Phys 2009;113:515–7.
[6] Liu Yanbin, Liu Zhiyi, Li Yuntao, Xia Qinkun, Zhou Jie. Mater Sci Eng A 2008;492:333–6.
[7] Kamp N, Gao N, Starink MJ, Sinclair I. Int J Fatigue 2007;29:869.
[8] Wang SC, Starink MJ. Int Mater Rev 2005;50:193.
[9] Ringer SP, Hono K, Sakurai T, Polmear IJ. Scr Mater 1997;36:517.
[10] Starink MJ, Wang SC. Acta Mater 2009;57:2376–89.
[11] Majimel J, Molenat G, Danoix F, Blavette D, Lapasset G, Casanove MJ. Mater Sci Forum 2002;239–402:1025.
[12] Wang SC, Starink MJ. Acta Mater 2007;55:933.
[13] Gupta AK, Gaunt P, Chaturvedi MC. Philos Mag A 1987;55:375.
[14] Alekseev AA, Anan'ev VN, Ber LB, Kaputkin EY. Phys Met Metallogr 1993;75:279.
[15] Li C, Yan M. Mater Sci Eng 1983;57:143.
[16] Ringer SP, Caraher SK, Polmear IJ. Scr Mater 1998;39:1559.
[17] Starink MJ, Gao N, Yan JL. Mater Sci Eng A 2004;387–389:222.
[18] Starink MJ, Cerezo A, Yan JL, Gao N. Philos Mag Lett 2006;86:243.
[19] Kovarik L, Court SA, Fraser HL, Mills MJ. Acta Mater 2008;56:4804–15.
[20] Starink MJ, Gao N, Davin L, Yan JL, Cerezo A. Philos Mag 2005;85:1395.
[21] Perlitz H, Westgren A. Arkiv Kemi Mineral Geol 1943;16B:13.
[22] Klobes B, Staab TE, Dudzik E. Phys Stat Sol – Rapid Res Lett 2008;2:182–4.
[23] Starink MJ. Int Mater Rev 2004;49:191–226.
[24] Starink MJ, Gao N, Davin L, Yan J, Cerezo A. Phil Mag 2005;85:1395–418.
[25] Khan IN, Starink MJ. Mater Sci Technol 2008;24:1403–10.

Please cite this article in press as: Parel TS et al. Hardening of an Al–Cu–Mg alloy containing Types I and II S phase precipitates. J Mater Design (2010), doi:10.1016/j.matdes.2009.12.048